Terms of use:

23/04/2024 22:28

(Article begins on next page)
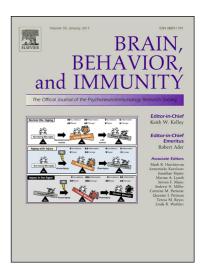
Accepted Manuscript

LPS-induced histone H3 phospho(Ser10)-acetylation(Lys14) regulates neuronal and microglial neuroinflammatory response

Giovanna Rigillo, Antonietta Vilella, Cristina Benatti, Laurent Schaeffer, Nicoletta Brunello, Johanna M.C. Blom, Michele Zoli, Fabio Tascedda

Please cite this article as: Rigillo, G., Vilella, A., Benatti, C., Schaeffer, L., Brunello, N., Blom, J.M.C., Zoli, M., Tascedda, F., LPS-induced histone H3 phospho(Ser10)-acetylation(Lys14) regulates neuronal and microglial neuroinflammatory response, *Brain, Behavior, and Immunity* (2018), doi: https://doi.org/10.1016/j.bbi.2018.09.019

LPS-induced histone H3 phospho(Ser10)-acetylation(Lys14) regulates neuronal and microglial neuroinflammatory response

Giovanna Rigillo[a,1], Antonietta Vilella[b,c,1], Cristina Benatti[a,c], Laurent Schaeffer[d], Nicoletta Brunello[a,c], Johanna M.C. Blom[e,c], Michele Zoli[b,c,2], Fabio Tascedda[a,c,2,*]

[a]Department of Life Sciences, University of Modena and Reggio Emilia, Via Campi 287, 41125, Modena, Italy

[b]Department of Biomedical, Metabolic and Neural Sciences, University of Modena and Reggio

[c]Center for Neuroscience and Neurotechnology, University of Modena and Reggio Emilia, Modena, Italy

[d]Institut NeuroMyoGene, CNRS UMR5310, INSERM U1217, Université Lyon1, 46 Allée d'Italie, 69007, Lyon, France

[e]Department of Education and Human Sciences, University of Modena and Reggio Emilia, viale Antonio Allegri 9, 42121 Reggio Emilia, Italy

[1] Both authors contributed equally to this work.

[2] Both authors contributed equally to this work.

* Corresponding author: fabio.tascedda@unimore.it (F. Tascedda)

Word count: 7362

Abstract

Epigenetic modifications of DNA and histone proteins are emerging as fundamental mechanisms by which neural cells adapt their transcriptional response to environmental cues, such as, immune stimuli or stress. In particular, histone H3 phospho(Ser10)-acetylation(Lys14) (H3S10phK14ac) has been linked to activation of specific gene expression. The purpose of this study was to investigate the role of H3S10phK14ac in a neuroinflammatory condition. Adult male rats received a intraperitoneal injection of lipopolysaccharide (LPS) (830 µg/Kg/i.p., n=6) or vehicle (saline 1mL/kg/i.p., n=6) and were sacrificed 2 or 6 h later. We showed marked region- and time-specific increases in H3S10phK14ac in the hypothalamus and hippocampus, two principal target regions of LPS. These changes were accompanied by a marked transcriptional activation of interleukin (IL) 1β, IL-6, Tumour Necrosis Factor (TNF) α, the inducible nitric oxide synthase (iNOS) and the immediate early gene c-Fos. By means of chromatin immunoprecipitation, we demonstrated an increased region- and time-specific association of H3S10phK14ac with the promoters of IL-6, c-Fos and iNOS genes, suggesting that part of the LPS-induced transcriptional activation of these genes is regulated by H3S10phK14ac. Finally, by means of multiple immunofluorescence approach, we showed that increased H3S10phK14ac is cell type-specific, being neurons and reactive microglia, the principal histological types involved in this response.

Present data point to H3S10phK14ac as a principal epigenetic regulator of neural cell response to systemic LPS and underline the importance of distinct time-, region- and cell-specific epigenetic mechanisms that regulate gene transcription to understand the mechanistic complexity of neuroinflammatory response to immune challenges.

1. Introduction

Numerous studies on animal models have shown that systemic inflammatory stimuli, such as administration of lipopolysaccharide (LPS), trigger an inflammatory response in the brain, despite the presence of the blood-brain barrier, resulting in microglial cell activation and increased expression and release of inflammatory cytokines that can persist long after peripheral events have subsided (Cunningham, 2013; Qin et al., 2007). In response to a pathogen, activated innate immune cells in the periphery produce pro-inflammatory mediators such as the cytokines interleukin (IL) 1β, IL-6, and Tumour Necrosis Factor (TNF) α and nitric oxide (NO) that can act also within the brain resulting in a strong effect on neuroinflammation (Henry et al., 2009; Sierra et al., 2007). This exaggerated pro-inflammatory response can be neurotoxic, can lead to behavioral alterations and exacerbate pathological processes leading to neurodegenerative and neuropsychiatric diseases (Benatti et al., 2016; Godbout et al., 2005; Layé et al., 1994; Matt et al., 2016; Qin et al., 2007). Inflammatory mediators seem to act at different levels in the central nervous system (CNS) and determine profound alterations in neurological and endocrine functions, particularly in the areas of the limbic system (Alboni and Maggi, 2015; Godbout et al., 2005; Layé et al., 1994; Qin et al., 2007). The hypothalamus and hippocampus are key structures for brain cytokine expression and function (André et al., 2008; Gądek-Michalska et al., 2013; Lynch, 2002) and are implicated in the neurobiological mechanisms underlying the behavioral, cognitive, emotional, and motivational alterations of cytokine-induced sickness behavior as well as the physiological response to acute infection (André et al., 2008; Dantzer, 2009; Frenois et al., 2007; Lupien et al., 2009). Specifically, the hypothalamus participates in the control of the hypothalamus-pituitary-adrenal (HPA) axis activity and in the stress response and coordinates physiological functions such as sleep and feeding, known to be altered in the cytokine-induced sickness syndrome (Alboni et al., 2013a; Silvia Alboni

3

et al., 2017; Basta-Kaim et al., 2011; Damm et al., 2012; Fletcher et al., 2010; Francesconi et al., 2016; Gore, 2010). The hippocampus, that subserves important functions such as spatial learning and memory, is strongly affected by immune challenges as well (Alboni et al., 2013b; Arai et al., 2001; Benatti et al., 2011; Lupien et al., 2009; Nabavi et al., 2016).

Emerging observations suggest that patterns of gene expression induced by neuroinflammation are activated or silenced through alterations of the chromatin structure (Claycombe et al., 2015; McClung and Nestler, 2008). Epigenetic modifications of both DNA and histone proteins are now accepted as fundamental mechanisms by which neural cells adapt their transcriptional response to developmental and environmental cues (Bagot et al., 2014; Nestler, 2014). Epigenetic regulation may influence gene expression through stable, long-term modifications that involve DNA methylation, or through a more flexible (short-term) way that involves histone modifications, such as phosphorylation and acetylation (Chen et al., 2002; Garden, 2013; Handy et al., 2011; Weaver et al., 2004; Zhou et al., 2011). In particular, the present study was focused on a specific histone modification, the simultaneous phosphorylation on the residue of Serine-10 (S10) and acetylation on the residue of Lysine-14(K14) in the N-terminal of the histone H3.

Phospho(S10)-acetylation(K14) of histone H3 (H3S10phK14ac) is dynamic and reversible and could serve to amplify the readout of upstream signaling pathways causing greater changes in the overall charge density of tails that resulting in greater modification of the chromatin structure of target genes (Colvis et al., 2005; Nowak and Corces, 2000; Rea et al., 2000; Thompson et al., 2001). Further evidence showed an increase of H3 phosphorylation in hippocampal neurons after seizures, that occurs in the c-Fos promoter region determining an elevation of c-Fos gene expression (Clayton et al., 2000; Mori et al., 2013). c-Fos is one of the most widely studied target genes because it is critical for synaptic plasticity and hippocampal memory (Alboni et al., 2017; Fleischmann et al., 2003; He et al., 2002; Tischmeyer and Grimm, 1999). Recent studies demonstrated that neuronal activity

induces the formation of DNA double-strand breaks, also within the promoters of early-response genes, such as c-Fos, facilitating their expression (Corbett et al., 2017; Madabhushi et al., 2015; Olsson et al., 2009; Watson and Tsai, 2017).

Little is known about the role of histone modifications in regulating transcription of specific genes involved in neuroinflammation. Recent studies suggest H3S10phK14ac capacity to activate transcriptional response and evidence shows the induction of H3S10phK14ac after administration of LPS in an invertebrate model (Garden, 2013; Ottaviani et al., 2013). It was also demonstrated that LPS-induced phosphorylation (S10) and phospho-acetylation (S10/K14) of H3 histone are crucial for recruiting the transcription factor NF-κB to the promoter of specific cytokines genes, such as IL-12 (Hamon and Cossart, 2008; Saccani et al., 2002).

Based on this knowledge, the purpose of this work was to demonstrate the regulation by H3S10phK14ac of pro-inflammatory gene expression in a rat model of neuroinflammation, focusing the study on the cellular populations more involved in the inflammatory response and epigenetic mechanisms.

2. MATERIAL AND METHODS

2.1. Animals and treatment

Adult male rats (Sprague-Dawley, Charles-River Laboratories, Calco (LE), Italy) were used in this study. Animals were housed in polycarbonate cages with ad *libitum* access to food and water throughout the study and maintained under a 12:12 light–dark cycle in an ambient temperature of 21±3°C with relative humidity controlled. The procedures used in this study were in strict accordance with European legislation on the use and care of laboratory animals (EU directive 2010/63/EU), with the guidelines of the National Institutes of Health on the use and care of laboratory animals (NIH Publications No.8023) and had the approval of the Italian Ministry of Health and of the local Ethical Committee. All efforts were made to minimize animal suffering and to reduce the number of animals used in this study. LPS (830 µg/Kg/mL, *Escherichia Coli* serotype 0127:B8, Sigma Aldrich L3129) was injected intraperitoneally (i.p.) and an equal volume of vehicle (saline) was used as a control. The dose of LPS was selected on the basis of its ability to induce sickness behavior and cytokine expression in the periphery and in the brain (Dantzer et al., 2008; Dantzer and Kelley, 2007; Lawson et al., 2013; Layé et al., 1994). Animals were sacrificed 2 h or 6 h after injection, hippocampi and hypothalamus were harvested, immediately frozen on dry ice, and stored at -80°C until further molecular analysis.

2.2. Cell cultures and treatments

The mouse clonal hippocampal neuronal cell line HT-22 was a generous gift from Dr. Maher Pamela (The Salk Institute for Biological Studies, La Jolla, San Diego, CA). The murine microglial cells BV-2 were obtained from Professor Samuele Peppoloni (University of Modena and Reggio Emilia, Modena, Italy). Cells were maintained at 37°C and 5% CO_2 in complete medium containing DMEM High glucose for HT-22, or RPMI 1640 for BV-2, supplemented with 10% heat-inactivated (56°C, 30

6

min) fetal bovine serum (FBS Gibco® Italy, Milan), 50 U/ml penicillin, 50mg/ml streptomycin and passed by tripsinization. Cells ($2x10^6$) were seeded into Petri dishes and grown for 20-24 h until 70-80% confluent for protein analysis. For gene expression analysis cells were plated at a density of $1x10^6$ cells per well on 6-well plates in 2 mL of complete medium and treated the day after plating. Cells were harvested 2, 6 or 24 h after treatment with 100 ng/mL of LPS (*Escherichia Coli* serotype 0127:B8, Sigma Aldrich L3129), while the control group received phosphate-buffered saline (PBS). Two independent experiments were performed.

2.3. Protein extraction

The hippocampus and hypothalamus of LPS-treated (n=6) and saline-treated (n=6) rats were homogenized by a potter (30 strokes at 60 rpm) in a volume 20 times the weight of tissue of Lysis Buffer (10 mM Hepes, 0.1 mM EGTA, 0.28 M Sucrose containing protease inhibitor Complete (Roche) and phosphatase inhibitor (10 µL Na_3VO_4, 50 µL NaPP, 20 µL NaF).

A fraction of the lysate was collected (total extract) and the remaining fraction was centrifuged at 1500 g for 5 min at 4°C. The supernatant was collected (cytoplasm fraction) and the pellets were resuspended in a Low Salt Buffer (20 mM Hepes, 2 mM $MgCl_2$, 0.1 M KCl, 25% Glycerol, 5 mM Dithiothreitol (DTT)). The fraction was centrifuged at 1500 g for 5 min at 4°C. The supernatant was discarded, and the pellets were resuspended in a High Salt Buffer (20 mM Hepes, 2mM $MgCl_2$, 1M KCl, 1mM EDTA, 25% Glycerol, 5 mM DTT), then vortexed vigorously and kept in ice for 30 min. Finally, the lysate was centrifuged at 13200 rpm for 30 min at 4°C. The supernatant was collected, and the pellets were resuspended in a Resuspension Buffer (120 mM NaCl, 20 mM Hepes, 0.1 mM EGTA, 0.1 mM DTT, protease and phosphatase inhibitor) (nuclear enriched extract).

For protein extraction, HT-22 and BV-2 cells were resuspended in omogenization buffer and homogenized with 40 strokes in a Dounce homogenizer (loose pestle) (Incofar, Italy) as previously described (Alboni et al., 2014a).

7

Protein concentration was determined using standard protocol Coomassie® reagent (Thermo Fisher Scientific, Waltham, MA USA). Total, cytosolic and nuclear fractions were stored at -20°C.

2.4. Western blotting

Western blotting was carried out as previously described (Benatti et al., 2018) on 4 µg of nuclear enriched extract of tissues and 10 µg of nuclear extract of cells for phospho(S10)-acetyl(K14) histone H3, phospho(S10)-histone H3,total histone H3. Overnight incubation at 4°C was with the following primary antibodies: anti-phospho(S10)-acetyl(K14) histone H3 (1:1000, Millipore®, #07-081); anti-phospho(S10) histone H3 (1:1000, Millipore, #06-570); anti-histone H3 (1:1000, Millipore®, #06-755) in blocking-buffer. Secondary antibody: anti-rabbit IgG-HRP-linked (1:5000, Cell Signaling®, #7071) for all targets. The levels of protein were calculated by measuring the peak densitometric area of the autoradiography analyzed with an image analyzer. The optical densities (OD) of phospho(S10)-acetyl(K14) histone H3 and phospho(S10) histone H3 signals were expressed as ratio of the OD of total histone H3, run and detected on the same blot after stripping.

2.5. Total RNA extraction, reverse transcription, and real time polymerase chain reaction

RNA extraction and DNAse treatment were performed as previously described (Benatti et al., 2014) using GenElute™ Mammalian Total RNA Miniprep Kit and DNASE70-On-Column DNase I Digestion Set (Sigma Aldrich ®, Milan, Italy). Two µg of total RNA were reverse transcribed with High Capacity cDNA Reverse Transcription Kit (Thermo Fisher Scientific, Waltham, MA USA) and Real Time PCR was performed, as previously described (Benatti et al., 2018), in ABI PRISM 7900 HT (Thermo Fisher Scientific, Waltham, MA USA) using Power SYBR Green mix (Thermo Fisher Scientific, Waltham, MA USA) and specific forward and reverse primers at a final concentration of 150 nM (Table 1 for both *in vitro* and *in vivo* experiments). Cycle threshold (Ct) value was determined by the SDS software 2.2.2 (Thermo Fisher Scientific, Waltham, MA USA), mRNA expression was calculated with the ΔΔCt method with glyceraldehydes-3-phosphate dehydrogenase (GAPDH) as endogenous control.

2.6. ChIP and PCR analyses

Chopped hippocampus and hypothalamus of LPS (n=6) and saline (n=6) treated rats were cross-linked with 1% formaldehyde for 15 min then the reaction was stopped by adding 0.125M glycine for 5 min at RT. Fixed tissues were washed twice with ice-cold PBS and homogenized by potter (15 strokes at 60 rpm) in 1 mL of PBS in the presence of protease inhibitor Complete. Samples were centrifuged at 5000 rpm for 5 min at 4°C, pellet was resuspended in Cellular Lysis Buffer (10 mM Tris-HCl pH 8.0, 10 mM NaCl, 0.2% Igepal, protease and phosphatase inhibitors) and kept on ice for 15 min. The lysate was centrifuged at 5000 rpm for 5 min at 4°C then the supernatant was collected, and the pellet resuspended in Nuclear Lysis Buffer (50 mM Tris-HCl pH 8.0, 10 mM EDTA, 0.5 % SDS, protease and phosphatase inhibitors) and kept on ice for 30 min. The chromatin was sonicated 4 times (30 sec on/30 sec off) at 270 setting in Labsonic sonicator (B.Braun International®) to produce 500-1000bp fragments, then was centrifuged at 14000 rpm for 10 min. The protein concentration was measured using standard protocol Coomassie® reagent (Thermo Fisher Scientific, Waltham, MA USA). The volume of lysate for 1 µg/µL was diluted to a final volume of 2 mL in a mixture of 9 parts Dilution buffer (1.1% Triton X-100, 1.2 mM EDTA pH 8, 16.7 mM Tris-HCl pH 8 and 167 mM NaCl) and 1 part of Lysis buffer (1% SDS, 10 mM EDTA pH 8, 50 mM Tris-HCl pH 8) and pre-cleared for 2 h, rotating at 4°C, with 10 µL of protein G Agarose beads 50% slurry (KPL, Gaithersburg MD, USA). Samples were centrifuged at 2000 rpm for 5 min and the supernatant was incubated with 3 µL of the antibody anti-phospho(S10)-acetyl(K14) histone H3 (Millipore®, #07-081) overnight rotating at 4°C. Simultaneously, 10 µL of protein G beads were incubated with a pre-blocked mix consisting of 9:1 (Dilution: Lysis), 100 µg/mL BSA and 500 µg/mL sheared salmon sperm DNA in a final volume of 100 µL for each chromatin and rotated overnight at 4°C. After immuno-precipitation, 10 µL of protein G pre-blocked beads, previously washed, were added to each sample and incubated for 2 h while rotating at 4°C. The unbound material was recovered as input and beads were washed 3 times

with Wash Buffer (1% Triton X-100, 0.1% SDS, 150 mM NaCl, 2 mM EDTA pH 8.0, 20 mM Tris-HCl pH 8.0) and once with a Final Wash Buffer (1% Triton X-100, 0.1% SDS, 500 mM NaCl, 2 mM EDTA pH 8.0, 20 mM Tris-HCl pH 8.0). ChIPed material was eluted by two 15 min incubations at RT with 250 µL of Elution Buffer (1% SDS, 0.1 M NaHCO$_3$). Chromatins, including input samples, were cross-linked reverse and DNA was submitted to RNAse and proteinase K digestion by incubating first at 37°C for 1 h, then at 65°C for 4 h minimum, and finally extracted by phenol-chloroform. Immuno-precipitation reactions were performed in duplicate using a no-antibody sample as a non-specific control. Immunoprecipitated DNA and inputs of hypothalamus and hippocampus were analyzed by a gradient PCR analysis using GoTaq® Flexi DNA Polymerase (Promega® Italia, Milan, Italy).

The promoter region of the gene of interest was amplified using specific primers as reported in Table 1. PCR results were analyzed by ImageJ software: each immuno-precipitated chromatin was normalized to the corresponding total chromatin (input).

2.7. Sample preparation for histology

For histological processing, animals were anesthetized with chloral hydrate (400 mg/kg, i.p.). Intracardial perfusion was performed with 4% paraformaldehyde and 0.2% picric acid in Phosphate Buffered Saline (PBS) (100mL/15min) preceded by an infusion of 50 mL of 0.9% NaCl saline containing heparin sodium (5000U/L); then, brains were dissected out. The brains were post-fixed in the same solution for 12 h, rinsed in 15% PBS-sucrose for approximately 12 h and then in a 30% PBS-sucrose for 1 day. The brains were frozen using dry ice, and coronal 50 µm thick sections series were cut at a cryotome, washed three times in cold PBS and stored at -20°C in a glycerol-PBS solution until use.

2.8. Immunohistochemistry

Brain sections of LPS (n=6) and saline (n=6) treated rats were processed for multiple immunofluorescence histochemistry as previously described (Vilella et al., 2014). Briefly, after five

10 min washes with PBS pH 7.4, blocking was performed for 1 h at RT in PBS containing 0.1% TritonX100, 1% bovine serum albumin (BSA). Rabbit anti-phospho(S10)acetyl(K14) histone H3 (Millipore®, #07-081), mouse anti-neuronal nuclear protein (NeuN, Millipore®, #MAB377), mouse anti-ionized calcium binding adapter molecule 1 (Iba1, Millipore®, #MABN92), anti-glial fibrillary acidic protein (GFAP, Dako, #M076) primary antibodies were diluted in PBS containing 0.3% TritonX100, 1% normal goat serum (NS) and incubation was performed overnight at 4°C. Before incubation with mouse anti-NeuN, brain sections were treated with citrate buffer (10mM Citric Acid, 0.05% Tween 20, pH 6.0) for 20 min at 98°C, then 20 min at RT. After three washes in 0.1% PBS-Triton X100, incubation with goat anti mouse Alexa Fluor 488 or goat anti-rabbit Alexa Fluor 546 secondary antibody diluted in PBS containing 0.2% Triton X100, 1% NS was carried out for 90 min at RT. After washing three times with PBS for 10 min, brain sections were placed on gelatinized glass slides, dried and, after incubation with DAPI, mounted for confocal microscopy analysis.

2.9. Statistical analysis

Statistical analysis was performed by means of two-way analysis of variance (ANOVA) using treatment group and time as factors. In case of significant effects, further comparisons between LPS- and vehicle- treated groups were performed by means of one-way ANOVA. $p < 0.05$ was considered as a threshold for significant difference.

For gene expression analysis, the mRNA levels of each target were normalized to the endogenous control, GAPDH. Endogenous control mRNA levels were not affected by any treatment ($p > 0.05$, One-way ANOVA). For quantitative evaluation of changes the comparative ΔΔCt method was performed, using as calibrator the average levels of expression of vehicle-receiving animals sacrificed 2 h after injection.

For ChIP analysis, quantitative enrichment of LPS sample, compared to control sample, was statistically performed by means of an independent Student's *t*-test and expressed in fold changes.

11

No difference was observed in both expression and protein levels of the evaluated targets between vehicle treated animals sacrificed 2 or 6 h after the injection (p>0.05).

Statistical analysis for *in vitro* results was performed by means of one-way ANOVA followed by Dunnett's post hoc test.

Data are presented as mean ± standard error of the mean (S.E.M.). Analyses were conducted using SPSS for Windows® v.25 (SPSS Inc., Chicago, USA).

3. RESULTS

3.1 Systemic LPS induces the expression of the pro-inflammatory cytokines IL-1β, IL-6, and TNF-α, the enzyme iNOS, and the immediate early gene c-Fos in rat hypothalamus and hippocampus.

In order to ensure the effectiveness of LPS (830 µg/Kg, i.p.) in stimulating the immune system and induce an inflammatory condition in the CNS, the expression levels of the major pro-inflammatory cytokines known to be produced within the brain, such as IL-1β, IL-6 and TNF-α, were measured in the rat hypothalamus and hippocampus 2 and 6 h after a systemic LPS challenge (Dantzer, 2009; Dantzer et al., 2008).

In the hypothalamus, IL-1β, IL-6 and TNF-α mRNA levels markedly increased after LPS injection. The statistical analysis showed that IL-1β significantly increased at both 2 and 6 h time intervals by about 70 and 80 times, respectively (Fig. 1A) (*two-way ANOVA*, IL-1β Treatment $F_{(1,18)}$=79.907, p<0.001; Time $F_{(1,18)}$=0.569, p=0.460; Treatment*Time $F_{(1,18)}$=0.584, p=0.454; LPS Vs. vehicle, 2h: p<0.001, 6h: p=0.002), while IL-6 and TNF-α expression levels were significantly increased at 2 h (by about 30 and 6 times, respectively) and underwent a further increase at 6h (by about 60 and 9 times, respectively) (Fig. 1B and C) (IL-6: Treatment $F_{(1,18)}$=44.841, p<0.001; Time $F_{(1,18)}$=4.116, p=0.058; Treatment*Time $F_{(1,18)}$=3.999, p=0.061; LPS Vs. vehicle, 2h: p<0.001, 6h: p=0.004; TNF-α: Treatment $F_{(1,18)}$=139.950, p<0.001; Time $F_{(1,18)}$=11.484, p=0.003; Treatment*Time $F_{(1,18)}$=10.070, p=0.005; LPS Vs. vehicle, 2h: p<0.001, 6h: p<0.001).

A LPS-induced increase in the levels of the three cytokine mRNAs was observed also in the hippocampus with a different pattern of change with respect to the hypothalamus. IL-1β mRNA levels significantly increased at 2 h (about 7 times) and much more at 6 h (about 60 times) (Fig. 1A) (*two way-ANOVA*, Treatment $F_{(1,18)}$=14.760, p<0.001; Time $F_{(1,18)}$=9.877, p=0.006; Treatment*Time $F_{(1,18)}$=9.907, p=0.006; LPS Vs. vehicle, 2h: p=0.001, 6h: p=0.013). IL-6 expression was significantly increased by about 4 and 6 times at 2 and 6 h, respectively (Fig. 1B) (Treatment

F(1,18)=24.353, p<0.001; Time F(1,18)=1.878, p=0.187; Treatment*Time F(1,18)=0.887, p=0.359; LPS Vs. vehicle, 2h: p=0.015, 6h: p=0.004). Hippocampal TNF-α mRNA levels significantly increased only at 6h by about 20 times (Fig. 1C) (Treatment F(1,18)=22.487, p<0.001; Time F(1,18)=20.762, p<0.001; Treatment*Time F(1,18)=21.473, p<0.001; LPS Vs. vehicle, 2h: p=0.484, 6h: p=0.003).

Subsequently, we investigated the mRNA levels of the inducible nitric oxide synthase (iNOS) which plays an important role in the response to pathogens, as well as in tumor growth, and produces NO upon stimulation by pro-inflammatory cytokines such as IL-1 and TNF-α (Carreira et al., 2015; Moraes et al., 2006; Satta et al., 1998). In both the hypothalamus and hippocampus, highly significant increases in iNOS transcript levels were detected at 2 h (about 110 and 50 times, respectively) and were further increased at 6 h (about 800 and 230 times, respectively) after LPS injection (Fig. 1D) (hypothalamus: Treatment F(1,18)=142.971, p<0.001; Time F(1,18)=82.158, p<0.001; Treatment*Time F(1,18)=82.657, p<0.001; LPS Vs. vehicle, 2h: p=0.001, 6h: p<0.001; hippocampus: Treatment F(1,18)=32.678, p<0.001; Time F(1,18)=13.361, p=0.002; Treatment*Time F(1,18)=13.254, p=0.002; LPS Vs. vehicle, 2h: p=0.014, 6h: p=0.002).

Finally, we tested the effects of LPS on the expression of the immediate early gene c-Fos, which is considered to be a marker of neuronal activity and shown to be induced after the activation of the peripheral innate immune system in a rapid and transient manner in different brain areas proposed to be involved in the cytokine-induced sickness response. Though less intense than for cytokines and iNOS, a significant increase of c-Fos mRNA levels was detected at both 2 and 6 h (about 3.5 and 3 times, respectively) after LPS injection in the hypothalamus, whereas no significant change was detected in the hippocampus (Fig. 1E) (hypothalamus: Treatment F(1,18)=29.816, p<0.001; Time F(1,18)=1.083, p=0.312; Treatment*Time F(1,18)=0.169, p=0.686; LPS Vs. vehicle, 2h: p<0.001, 6h: p=0.020; hippocampus: Treatment F(1,18)=1.221, p=0.284; Time F(1,18)=1.730, p=0.205; Treatment*Time F(1,18)=1.478, p=0.240).

3.2 Systemic LPS induces phosphorylation (S10) and phospho(S10)-acetylation(K14) of histone H3 in the rat hypothalamus and hippocampus.

We measured, by western blot, the effects of an inflammatory stimulus on the levels of histone H3 phosphorylation (S10) (H3S10ph) and H3S10phK14ac in the nuclear fractions extracted from the rat hypothalamus and hippocampus 2 and 6 h after the systemic administration of LPS (830 μg/Kg, i.p.). In both the hypothalamus and hippocampus, a significant increase of H3S10phK14ac levels was detected 2 h after LPS treatment, whereas at 6 h H3S10phK14ac levels were markedly decreased in both regions though a trend for a significant increase was still present in the hypothalamus (Fig. 2A and B) (hypothalamus: Treatment $F_{(1,16)}=15.843$, $p=0.001$; Time $F_{(1,16)}=19.941$, $p<0.001$, Treatment*Time $F_{(1,16)}=4.751$, $p=0.045$; LPS Vs. vehicle, 2h: $p=0.001$, 6h: $p=0.054$; hippocampus: Treatment $F_{(1,19)}=26.899$, $p<0.001$; Time $F_{(1,19)}=53.393$; $p<0.001$, Treatment*Time $F_{(1,19)}=27.781$; $p<0.001$, LPS Vs. vehicle, 2h: $p=0.001$, 6h: $p=0.875$). In both regions, LPS treatment did not modify total H3 protein levels (data not shown). A partially different effect was observed for H3S10ph. In this case, in both hypothalamus and hippocampus, LPS treatment induced a significant increase in H3S10ph levels at 2 and 6 h (Fig. 3A and B) (hypothalamus: Treatment $F_{(1,16)}=44.788$, $p<0.001$; Time $F_{(1,16)}=0.250$, $p=624$; Treatment*Time $F_{(1,16)}=3.008$, $p=0.102$; LPS Vs. vehicle, 2h: $p<0.001$, 6h: $p=0.009$; hippocampus: Treatment $F_{(1,18)}=13.374$, $p=0.002$; Time $F_{(1,18)}=8.895$, $p=0.355$; Treatment*Time $F_{(1,18)}=0.590$, $p=0.451$; LPS Vs. vehicle, 2h: $p=0.016$, 6h: $p=0.049$).

3.3 Histone H3 phospho(S10)-acetylation(K14) is a mediator of the transcriptional response induced by LPS-challenge.

It has been suggested that the status of a chromatin region is coded by the combination of differentially modified histone tails (Sawicka and Seiser, 2012). Among these modifications, H3S10phK14ac results in transcriptional activation by opening chromatin conformation (Chen et al., 2002; Cheung et al., 2000; Tsankova et al., 2004). Here we hypothesized that LPS-induced

15

transcriptional activation of IL-1β, IL-6, iNOS or c-Fos genes may be regulated by the phospho-acetylation status of histone H3. Therefore, we evaluated the association of H3S10phK14ac to the promoter region of IL-1β, IL-6, iNOS, and c-Fos genes through ChIP experiments. Results showed that H3S10phK14ac was able to regulate the LPS transcriptional response in a time- and region-specific manner.

Two h after LPS administration, in the hypothalamus, PCR analysis showed a strong increase in H3S10phK14ac association to iNOS and c-Fos promoters compared to vehicle (t = 33.304, p=0.0009 and t=21.638, p=0.002, respectively) (Fig. 4A). A mild increase was observed for IL-6 gene (t=20.684, p=0.002) (Fig. 4A), while no change in H3S10phK14ac association was found for IL-1β (Fig. 4A). On the other hand, ChIP analysis in the hippocampus highlighted an H3S10phK14ac enrichment of over 10 times only to iNOS promoter after LPS administration when compared to vehicle-receiving counterparts (t=53.069, p=0.0004) (Fig. 4B).

Six h post LPS exposure, in the hypothalamus, PCR results showed an increased association of H3S10phK14ac to iNOS gene approximately 6 times greater than what was observed in the vehicle group (t=40.669, p=0.0006) (Fig. 4C). Instead, no changes in binding of H3S10phK14ac was detected for IL-1β, IL-6 and c-Fos gene promoters (Fig. 4C). Similarly, in the hippocampus, no alteration was found in H3S10phK14ac association to the promoters of any of the target genes examined (Fig. 4D). All samples were compared to total chromatin (input) and to the negative control without antibody (Fig. 4 A-D).

3.4. Cell-specific LPS-induced increase in histone H3 phospho(S10)-acetylation(K14).

Recent reports have clearly demonstrated significant differences in epigenetic modification patterns between neuronal and non-neuronal cells (Bousiges et al., 2013; Matt et al., 2016; Mori et al., 2013). Therefore, we decided to assess what cell types express increased H3S10phK14ac levels upon systemic exposure to LPS. In particular, neurons, astrocytes and microglial cells in rat hypothalamus

and hippocampus were analyzed by immunostaining with cell-specific antibodies including the neuron-specific anti-NeuN, the astroglia-specific anti- GFAP, and the microglia-specific anti-Iba-1. Scattered H3S10phK14ac immunoreactive nuclei were detected in several hypothalamic nuclei of control rats (see, Fig. 5A, D, G and Fig. 6A, D, G). A clear increase in nuclear H3S10phK14ac immunoreactivity was observed after LPS administration, though with different patterns of change in the different hypothalamic nuclei. In the magnocellular paraventricular nucleus, positive nuclei markedly increased at 2 h and further increased at 6 h (not shown). In the parvocellular paraventricular (Fig. 5) and periventricular (not shown) nuclei, the marked increase at 2 h (Fig. 5B, E, H) was followed by a slight decrease at 6 h (Fig. 5C, F, I). Finally, in the arcuate nucleus, the sharp increase of H3S10phK14ac positive signal at 2 h was followed by a marked decrease at 6 h, that did not, however, reach control levels (not shown). A clear increase in H3S10phK14ac immunoreactivity was also observed in ependymal cells of the III ventricle (Fig. 6) both at 2 (Fig. 6B, E, H) and 6 h (Fig. 6C, F, I) after LPS administration as well as in vascular endothelial cells (not shown).

In double immunofluorescence experiments using antibodies against H3S10phK14ac and cell-specific markers, we could identify the cellular identity of the H3S10phK14ac immunoreactive nuclei. The large majority of H3S10phK14ac immunoreactive nuclei co-expressed NeuN immunoreactivity and were therefore identified as neuronal nuclei (Fig. 7A, B). Instead, we could not identify clear-cut instances of co-localization between H3S10phK14ac immunoreactivity and the nuclei of astroglial cells, identified by GFAP immunoreactivity, in hypothalamic nuclei (not shown). Finally, regarding the nuclei of microglial cells, identified by Iba-1 immunoreactivity, a moderate level of H3S10phK14ac/Iba-1 co-localization was detected at 2 h in some cells of the hypothalamus (Fig. 7C). Instead, several instances of H3S10phK14ac/Iba-1 co-localization were detected at 6h in the hypothalamic nuclei examined (e.g., paraventricular, periventricular, and arcuate nuclei) (Fig. 7D). These latter microglial cells showed an amoeboid/phagocytic form. The intensity of

17

H3S10phK14ac immunoreactivity in Iba-1 positive nuclei was generally lower than the intensity of H3S10phK14ac immunoreactivity in NeuN-positive nuclei, with the exception of a few H3S10phK14ac/Iba-1 double immunoreactive cells with very intense H3S10phK14ac immunoreactivity. Notably, these latter microglial cells were in close proximity to ependymal cells of the ventricles and putative vascular endothelial cells (Fig. 7D).

In the hippocampus, dispersed H3S10phK14ac immunoreactive nuclei were detected in control rats all along the different subregions and layers (not shown). Two h after LPS, a sharp increase in H3S10phK14ac immunoreactive nuclei could be detected both in layers containing projection neurons (pyramidal and granule cell layers) and layers containing interneurons (Fig. 8A-C). At 6 h a decrease in H3S10phK14ac immunoreactivity was detected, in particular in pyramidal and granule cell layers (Fig. 8D-F). In all regions, several instances of H3S10phK14ac immunoreactive vascular endothelial cell nuclei were observed at both 2 and 6 h after LPS administration (not shown).

Double immunofluorescence experiments with cell type-specific markers, delineated a different pattern of staining of the principal cell types of the neural tissue. While only scattered NeuN cells showed H3S10phK14ac immunoreactivity in control rats, H3S10phK14ac/NeuN double immunoreactive cell nuclei markedly increased 2 h after LPS administration (Fig. 8A) and decreased at 6 h (Fig. 8D) without reaching control levels. We further analyzed the expression of H3S10phK14ac immunoreactivity in specific neuronal subpopulations expressing neuropeptide Y (NPY) or glutamic acid decarboxylase (GAD) immunoreactivity. We could detect both H3S10phK14ac/NPY and H3S10phK14ac/GAD double immunoreactive neurons at 2 h, that were no longer present at 6 h. H3S10phK14ac/GFAP double immunoreactive cells were rare in control rats and increased at both 2 and 6 h (Fig. 8G-J). Note that at 6 h H3S10phK14ac/GFAP double immunoreactive cells had a reactive phenotype. Finally, H3S10phK14ac/Iba-1 double immunoreactive cells were not detected in control rats (not shown) and 2 h (Fig. 8G) after LPS

administration but were clearly detected at 6 h (Fig. 8I) in some microglial cells with amoeboid/phagocytic form.

Overall, the analysis at cellular level showed a relatively heterogeneous pattern of change in the regions analyzed. Everywhere, however, neuronal cells appeared to be the predominant cell type expressing increased H3S10phK14ac immunoreactivity after LPS. Astroglial cells were absent or modestly positive in most areas (Fig. 8H, J), whereas several microglial cells with an amoeboid/phagocytic form showed H3S10phK14ac immunoreactivity in all the regions analyzed, especially 6 h after LPS administration.

3.5. Incubation with LPS elicits different effects on gene expression and nuclear H3S10phK14ac levels in hippocampal neuronal cell lines (HT-22) or murine microglia (BV-2)

We assessed IL-1β, IL-6, TNF-α, iNOS, and c-Fos transcription after a 2, 6, and 24 h exposure to LPS in HT-22 hippocampal neurons and BV-2 microglial cells (Fig. 9). One-way ANOVA revealed a main effect of incubation with LPS on mRNA levels of these targets in both cell lines, with Dunnett's post-hoc analysis showing a different time-dependent pattern for BV-2 and HT-22.

In BV-2, IL-1β and IL-6 were significantly induced at all the time points considered (by about 80, 150, and 120 times respectively for IL-1b and 100, 350, and 500 times for IL-6; One-way ANOVA, IL-1β: $F_{(3,17)}=1277.268$, $p<0.0001$; IL-6: $F_{(3,17)}=812.790$, $p<0.0001$) with respect to unstimulated controls (Fig. 9A, B). TNF-α mRNA was strongly increased in BV-2 following 2 or 6 h incubation with LPS, while at 24 h this effect, albeit still present, was decreased (increases by about 90, 50, and 10 times, respectively; TNF-α: $F_{(3,17)}=1107.617$, $p<0.0001$; Fig. 9C).

In hippocampal neurons IL-1β, IL-6, and TNF-α expression was significantly induced by a 2h exposure to LPS (by about 4, 20, and 14 times, respectively) with respect to untreated cells. No significant difference was found between LPS treated cells and unstimulated controls 6 or 24 h after LPS

incubation (IL-1β: $F_{(3,19)}=16.803$, p<0.0001; IL-6: $F_{(3,35)}=171.641$, p<0.0001; TNF-α: $F_{(3,31)}=42.903$, p<0.0001).

Also iNOS expression showed a distinct temporal pattern between neurons and microglia: in HT-22 cells iNOS was induced by about 1100 times as early as 2 h after LPS exposure ($F_{(3,35)}=99.139$, p<0.0001) with respect to untreated cells, while prolonging the incubation resulted in a decrease of this effect at 6 h, that was abolished at the 24 h time point (Fig. 9D). Conversely, in BV-2 cells the induction of iNOS expression by LPS with respect to unstimulated cells became statistically significant only after 6 h of exposure and was still present prolonging the incubation up to 24 h (by about 400 and 120 times, respectively; $F_{(3,17)}=1538.767$, p<0.0001).

c-Fos mRNA levels were significantly increased in both HT-22 and BV-2 cells only in the group exposed to LPS for 2 h but not following longer treatments ($F_{(3,30)}=77.606$, p<0.0001; $F_{(3,17)}=9.896$, p=0.002 respectively) (Fig. 9E).

We also measured, by western blot, the effects of a 2, 6 and 24 h incubation with LPS on the levels of H3S10phK14ac in the nuclear fractions of both HT-22 and BV-2 cell lines (Fig. 9F). One-way ANOVA revealed a main effect of LPS exposure on H3S10phK14ac levels in HT-22 ($F_{(3,23)}=4.351$, p=0.016) and BV-2 ($F_{(3,11)}=22.126$, p<0.0001). A significant increase of H3S10phK14ac levels was detected in LPS treated hippocampal neurons with respect to unstimulated controls at all the time points considered. When BV-2 murine microglia were exposed to LPS for 2 or 6 h, H3S10phK14ac levels were not different with respect to untreated cells, but a significantly increase (by about 3 times) was observed when the incubation lasted for 24 h. LPS treatment did not modify total H3 protein levels in either HT-22 or BV-2 cells (data not shown).

4. Discussion

The present study demonstrated that a systemic (i.p.) administration of LPS affects the hypothalamic and hippocampal transcription of pro-inflammatory targets in an area-specific and

20

time-dependent manner through specific epigenetic mechanisms. In particular, we demonstrated that the histone modification H3S10phK14ac is rapidly induced 2 h after the inflammatory challenge, decreases at 6 h post-LPS and is differentially regulated in cell populations of the areas analyzed. ChIP results indicated that LPS was able to induce active chromatin remodeling by H3S10phK14ac modification at c-Fos, IL-6, and iNOS gene promoter in a region- and time-dependent manner. This suggests that phospho(S10)-acetylated(K14) histone H3 transcriptional regulation induced by LPS is, at least in part, responsible for the observed very high increase in hypothalamic and hippocampal iNOS transcript and for the lower increase of c-Fos and IL-6 transcripts in the hypothalamus.

As expected, LPS increased the expression of the main pro-inflammatory cytokines in the hippocampus and hypothalamus (Alboni et al., 2014b; Damm et al., 2012; Dantzer, 2009; Layé et al., 1994; Lynch, 2002), however its effects on IL-1β, IL-6, TNF-α mRNA levels showed distinct changes in the two brain areas. In particular, we observed a stronger induction in the hypothalamus than in the hippocampus. We also demonstrated a time dependent massive increase of the levels of mRNA coding for the iNOS gene. The mRNA coding for the enzyme responsible of NO synthesis was enhanced 2 h after LPS injection in both areas, and this effect was still present and further increased 6 h post-injection. Expression of c-Fos, a marker of activated neurons, was markedly induced 2 and 6 h following the LPS challenge in the hypothalamus while no effect was observed in the hippocampus. Transcriptional effects on immediate-early genes suggest distinct temporal patterns of brain reactivity following LPS exposure (S Alboni et al., 2017; da Silva et al., 2014; Frenois et al., 2007; Ryabinin et al., 1997). Consistently with our data, the hypothalamus appears to be recruited in the early phase of the response to LPS, as suggested by the strong induction of c-Fos expression and FosB immunoreactivity occurring within 6 h post-injection observed by Frenois and colleagues (Frenois et al., 2007), while the hippocampus, not recruited in terms of c-Fos expression at any of

the time points considered in the present paper, may mediate the delayed effect of LPS, with changes occurring at a later stage.

H3S10phK14ac has been established to be an activating histone modification favouring specific gene transcriptional events (Clayton et al., 2000; Nowak and Corces, 2000). Increased H3S10phK14ac in the promoter regions of c-Fos in the brain has been demonstrated following other stimuli such as electroconvulsive seizures (Tsankova et al., 2004), administration of several neurotransmitter receptor agonists (Crosio, 2003), stress (Chandramohan et al., 2007; Collins et al., 2009). Present and previous evidence indicates that H3S10phK14ac is a crucial, though not necessary (Kumar et al., 2005), component of the epigenetic cascade driving c-Fos expression in the brain though other histone modifications may also contribute to the activatory regulation (Mifsud et al., 2011; Tsankova et al., 2004).

The causal link between H3S10phK14ac levels and target gene activation is reinforced by ChIP experiments that highlight that H3S10phK14ac increase precedes the peak of transcriptional activity of target genes and in parallel their temporal and regional heterogeneity. For instance, both H3S10phK14ac association to iNOS gene and iNOS mRNA levels are higher in hypothalamus than in hippocampus, and H3S10phK14ac association to c-Fos gene and increased c-Fos mRNA levels are only present in the hypothalamus.

In addition, LPS-induced changes in H3S10phK14ac are gene-specific since other genes, such as IL-1β and IL-6, whose mRNA levels are markedly increased by LPS treatment in both hypothalamic nuclei and hippocampus, did not show a significant association with H3S10phK14ac.

These data suggest that the two regions considered use different transcriptional regulation mechanisms in response to LPS stimulation. In hypothalamus the transcriptional activation of iNOS, IL-6, and c-Fos is bound, albeit to a different extent, to H3S10phK14ac levels on the promoter of these genes, whereas, in hippocampus, only iNOS promoter is upregulated after the inflammatory

insult, suggesting that in this region the transcriptional response to LPS administration follows different transcriptional dynamics, possibly involving other histone modifications or epigenetic mechanisms.

We observed also a significant increase in H3S10ph after LPS treatment as also demonstrated in other animal models of brain insult, such as kainate or pilocarpine induced-epilepsy (Mori et al., 2013; Taniura et al., 2006), depression (Bagot et al., 2014; Nestler, 2014) and ethanol exposure (McClain and Nixon, 2016; McClung and Nestler, 2008). After LPS challenge, increase in H3S10ph levels appeared less region- and time-dependent than H3S10phK14ac as it was increased by a similar extent in both hypothalamus and hippocampus at 2 and 6 h post-LPS injection. In fact, while H3S10ph in both areas is induced after 2 h and is still elevated even at 6 h, the H3S10phK14ac is attenuated at 6 h.

Notwithstanding the two histone modifications studied here have been shown to occur in a cooperative fashion, with phosphorylation of H3S10 promoting subsequent acetylation of H3K14 (Nowak and Corces, 2000), they are thought to positively regulate transcriptional processes targeting different genes and undergoing different post-stimulus changes (Chandramohan et al., 2007; James et al., 2012; Sawicka and Seiser, 2012). Accumulated data identified the MAPK/ERK cascade via mitogen- and stress-activated protein kinase (MSK) pathway as the mechanism mediating phosphorylation, acetylation and phosphoacetylation of histone H3 (Ciccarelli et al., 2013; Hamon and Cossart, 2008; Saccani et al., 2002; Soloaga et al., 2003; Thomson et al., 1999). The MAPK/ERK pathway results activated after different stimuli and its blockade, or the use of knockout cells for MSK1 and MSK2, leads to a marked reduction in the histone H3 phosphorylation, acetylation, and phospho-acetylation (Chwang et al., 2006; Soloaga et al., 2003).

Overall, present data suggest that H3S10phK14ac is a principal epigenetic mechanism that organizes the specific response to LPS of a large number of neuronal and non-neuronal cells. Cellular

23

distribution analyses indicate that in both hypothalamic nuclei and hippocampus, neuronal cells appear to be the main cell population responsible for the increase of H3S10phK14ac observed after LPS treatment. LPS administration is known to induce multiple neuroendocrine, autonomic and behavioral consequences, that include sickness behavior (hypolocomotion, social withdrawal, fatigue, anorexia, sleep pattern alterations), learning and memory deficits, and activation of the hypothalamus–pituitary–adrenal axis (Cunningham, 2013; Dantzer et al., 2008; Henry et al., 2009; Qin et al., 2007; Satta et al., 1998; Sens et al., 2017). This complex alteration of neuronal circuits tallies well with present evidence of extensive increased positivity for H3S10phK14ac, and the associated transcription activation, in many classes of neurons of hypothalamic and hippocampal circuits. Non-neuronal cells showed a sharp increase in H3S10phK14ac immunoreactivity even if the number of positive cells was more limited and heterogeneous compared to the number of positive neurons.

H3S10phK14ac immunoreactive microglial cells were visible both in hypothalamus and hippocampus though only a few of them were intensely positive and only at 6 h post-LPS injection. Notably, these microglial cells with intense positivity for H3S10phK14ac had an amoeboid/phagocytic form, that is typical of activated cells (Cherry et al., 2014). These data are in line with previous evidence on glial response to LPS. At early time points (first h after LPS), microglial activation has been repeatedly shown and is thought to contribute to both the inflammatory responses to LPS and the stimulation of neuron-mediated sickness behavior (Jin et al., 2016).

A few H3S10phK14ac immunoreactive astroglial cells were visible only in the hippocampus at 2 h and, as regards astrocytes with reactive morphology, at 6 h. A late activation of astrocytes tallies well with the evidence that cytokine expression and release by astrocytes peaks 12-24 h after LPS challenge and parallels the resolution of sickness behavior and microglial activation (Norden et al., 2016).

Besides glial cells, in the brain regions analyzed, other types of non-neuronal cells showed increased H3S10phK14ac levels, including ventricular ependymal cells and vascular endothelial cells. In fact, these cell types represent key components of the brain systems that monitor the presence of peripheral innate immune responses and trigger the associated alterations in brain circuits (Cheung et al., 2000; Dantzer et al., 2008).

The cell populations that showed the most intense H3S10phK14ac expression after LPS treatment were neurons and amoeboid, i.e., activated, microglia. Activated microglia become deramified and develop an enlarged cell body with several short, thickened processes. This morphological transformation occurs within hours from the initial activation and coincides with microglial homing and adhesion to damaged neurons (Kloss et al., 1999; Raivich et al., 1999). Microglia plays a fundamental regulatory role on neuronal function and homeostasis under physiological conditions, and it is thought that disruption of such fundamental processes upon an immune challenge or inflammation, may contribute to neuronal or synaptic dysfunction (Frick et al., 2013; von Bernhardi et al., 2015).

The time- and cell-specific pattern of H3S10phK14ac expression *in vivo* tallies well with our *in vitro* results showing a different pattern of regulation for H3S10phK14ac following LPS exposure between hippocampal neurons and microglia. While H3S10phK14ac levels were increased in neurons as early as after a 2 h exposure and remained elevated at least until 24 h in the hippocampal cell line HT-22, in microglia the phosphoacetylation of histone H3 was increased only after 24 h. Different transcriptional regulation mechanisms in response to LPS stimulation between BV-2 and HT-22 were confirmed by gene expression results as well. mRNA levels of genes related to the inflammatory response were strongly induced in HT-22 by LPS after a 2 h exposure and returned to basal levels following longer treatment, while for BV-2 cells the transcriptional effect of LPS was detectable even after exposure to LPS for 6 and 24 h. Future studies will be needed to dissect the role of

H3S10phK14ac in the transcriptional activation induced by LPS in different cell populations *in vivo* and *in vitro*, between HT-22 and BV-2.

iNOS hyperexpression is a principal molecular outcome of microglial activation since high concentrations of the radical molecule NO constitute a CNS cellular defense mechanism aimed at removing cellular debris and combating infection. However, excessive production of NO may induce neuroinflammation-mediated neuronal loss (Yuste et al., 2015). Accordingly, iNOS induction was shown to cause neuronal damage in the hippocampus leading to memory impairments (Abd El-Aleem et al., 2008; Carreira et al., 2015; Chuang et al., 2010; Luo et al., 2007), while in the hypothalamus it can lead to neuroendocrine responses to infection (McCann et al., 1997; Satta et al., 1998), insulin-resistance and consequent alteration in energy homeostasis observed in LPS-induced sickness behavior (Katashima et al., 2017; Ribeiro et al., 2013). Furthermore, in the same experimental condition, NO may activate the hypothalamic-pituitary-adrenal axis (Uribe et al., 1999). Besides microglia, also neurons and endothelial/ependymal cells may contribute to the observed increase in iNOS mRNA expression as already shown after traumatic brain injury, and oxygen and glucose deprivation (Heneka and Feinstein, 2001; Petrov et al., 2000; Rodrigo et al., 2001). In these cells, differently from microglial cells, H3S10phK14ac increased expression occurs rapidly and remains sustained at 6 h post-LPS injection, as confirmed also from our *in vitro* results. However, it is worth remembering that data from the literature suggest a different outcome for LPS on microglia activation depending on the route of administration, with centrally administered LPS inducing a clearer microglia activation than systemic LPS (Hoogland et al., 2015; Lawson et al., 2013). Present data clearly imply an epigenetic molecular mechanism based on increased H3S10phK14ac expression and association with iNOS gene in LPS-induced overexpression of iNOS in different cellular populations of both the hypothalamus and the hippocampus. This evidence adds on

previous studies showing the association of iNOS activation with specific chromatin modifications at the iNOS promoter observed in gastric cell after infection (Angrisano et al., 2012).

5. Conclusions

In this study we showed that a systemic LPS administration induces a marked region- and cell-specific phospho(S10)-acetylation(K14) of histone H3 (Fig. 10). LPS effects on H3S10phK14ac were cell population specific which emerged from both *in vitro* and *in vivo* experiments, even considering the limitations concerning the use of cell lines, as they do not always accurately replicate the features of native cells.

In addition, we propose that the increase in H3S10phK14ac may drive the transcription of some of the principal genes mediating LPS response in the brain, such as c-Fos, IL-6, and iNOS. Future experiments will focus on defining more complete molecular mechanisms which in turn will add to the generalizability of our findings. In particular, attention will also be directed to investigating which intracellular pathway mediates the effect of LPS on H3S10phK14ac and in determining a causal relationship between the transcriptional effects of LPS and histone H3 modifications by targeting *in vitro* phosphorylation of S10 or acetylation of K14.

The study underlines the importance of time-, region- and cell-specific epigenetic mechanisms that regulate gene transcription sustaining the neuroinflammatory response to an immune challenge.

FIGURE LEGENDS

Figure 1. Systemic LPS induces the expression of the pro-inflammatory cytokines IL-1β, IL-6, TNF-α, the enzyme iNOS, and the immediate early gene c-Fos in the rat hypothalamus and hippocampus. Adult male rats received either LPS (830 μg/Kg/i.p., n=6) or vehicle (saline 1mL/kg/i.p., n=6) and were sacrificed 2 or 6 h later. Interleukin (IL) 1β (A), IL-6 (B), Tumour Necrosis Factor (TNF) α (C), inducible nitric oxide synthase (iNOS) (D), and c-Fos (E) mRNA expression in the hypothalamus and hippocampus, with GAPDH as endogenous control, were measured by Real-time PCR. Data are represented as means ± S.E.M. and were analyzed with two-way ANOVA followed by one-way ANOVA for treatment Vs. control comparisons. *=p <0.05, **=p<0.01 LPS Vs. control.

Figure 2. Systemic LPS enhances the combined phospho(S10)-acetylation(K14) of histone H3 in the rat hypothalamus and hippocampus. A systemic injection of LPS (830 μg/Kg/i.p., n=6) enhanced H3S10phK14ac protein levels above those of control animals (saline 1mL/kg/i.p., n=6)(A) in both the hypothalamus and the hippocampus after 2 h, while at 6 h they returned to control values. Representative blots of H3S10phK14ac and H3 are shown (B). H3S10phK14ac protein levels were normalized to total histone H3 levels. Histone H3 protein levels did not significantly change. Each column represents mean ± S.E.M.. Data were analyzed with two-way ANOVA followed by one-way ANOVA for treatment Vs. control comparisons. **=p<0.01 LPS Vs. control.

Figure 3. Systemic LPS enhances the phosphorylation(S10) of histone H3 in the rat hypothalamus and hippocampus. H3S10ph protein levels increased 2 h after a systemic injection of LPS (830 μg/Kg/i.p., n=6) and remained elevated at 6 h in both the hypothalamus and the hippocampus with respect to control animals (saline 1mL/kg/i.p., n=6)(A). Representative blots of H3S10ph and H3 are shown (B). H3S10ph protein levels were normalized to total histone H3 levels. Histone H3 protein

levels did not significantly change. Each column represents mean ± S.E.M., data were analyzed with two-way ANOVA followed by one-way ANOVA for treatment Vs. control comparisons. *=p <0.05, **=p<0.01 LPS Vs. control.

Figure 4. **Phospho(S10)-acetyl(K14) histone H3 regulates LPS-induced transcriptional response**. ChIP analysis of the H3S10phK14ac enrichment on the promoter region of IL-1β, IL-6, iNOS, and c-Fos genes in LPS-treated (830 µg/Kg/i.p., n=6) and control rats (saline 1mL/kg/i.p., n=6). PCR analysis showed the H3S10phK14ac binding to c-Fos, iNOS, IL-1β, and IL-6 genes in hypothalamus 2 h after LPS administration (A). In hippocampus, at 2 h from the LPS treatment, a significant induction of iNOS gene transcription was observed by PCR (B). PCR results on the hypothalamus, 6 h after the LPS administration, display the effect of H3S10phK14ac only on the transcription of iNOS gene promoter (C). In the hippocampus of LPS-treated rats, PCR analysis on the ChIP fragments did not show alterations in the expression of IL-1β, IL-6, iNOS, and c-Fos promoters (D). Input samples represent the total of chromatin. No-antibody sample was used as negative control of the immunoprecipitation. Data were expressed as fold-changes of LPS-treated animals above the expression of control (saline injected) animals. Bars indicate the mean ± S.E.M.. Data were analyzed with Student's *t* test *p<0.01;**p<0.001 LPS Vs. control.

Figure 5. Phospho(S10)-acetyl(K14) histone H3 immunoreactivity in cell nuclei of parvocellular paraventricular nucleus of hypothalamus after LPS treatment. In panels A, B, C cell nuclei were stained with DAPI (blue). H3S10phK14ac (D-F, green) resulted to be increased in cells 2 (B,E,H) and 6 h (C, F, I) after LPS (830 µg/Kg/i.p., n=6) compared to control (saline 1mL/kg/i.p., n=6) (A, D, G). Merge images (G, H, I) show the co-localization of H3S10phK14ac with DAPI. Scale bar = 50 µm (A-I).

Figure 6. Phospho(S10)-acetyl(K14) histone H3 immunoreactivity in ependymal cells of the third ventricle after LPS treatment. In panels A,B,C cell nuclei were stained with DAPI (blue); H3S10phK14ac (D, E, F, green) resulted to be enhanced in ependymal cells 2 and 6 h after LPS (830 µg/Kg/i.p., n=6) compared to control (saline 1mL/kg i.p., n=6) (A,D,G). Ependymal cell layer is marked with white hatches. Merge images (G, H, I) show the co-localization of H3S10phK14ac with DAPI. Scale bar = 10 µm (A-I).

Figure 7. **Cell-specific localization of phospho(S10)-acetyl(K14) histone H3 immunoreactivity in the parvocellular paraventricular nucleus of hypothalamus**. Confocal microscopy images of brain cryosections labeled with DAPI (blue), H3S10phK14ac (red, panel A, B; green, panel C, D), NeuN (green, panel A, B) and Iba1 (red, panel C, D) are represented. Panels A and B show the colocalization between NeuN-positive neuronal nuclei and H3S10phK14ac immunoreactivity at both 2 and 6 h after LPS injection (830 µg/Kg/i.p., n=6). Panels C and D show a moderate and high level of H3S10phK14ac/Iba-1 co-localization, respectively, at 2 and 6h after LPS injection. Note that at 6h some microglial cells (yellow arrows) are in close proximity to putative vascular endothelial cells marked with white hatches. Scale bar = 10 µm (A-D).

Figure 8. Cell-specific localization of phospho(S10)-acetyl(K14) histone H3 immunoreactivity in the hippocampal dentate gyrus. Confocal microscopy images of brain cryosections labeled with DAPI (blue), H3S10phK14ac (red) and antibodies against different cell types (green) are represented. H3S10phK14ac (red) resulted to be enhanced in cells 2 h (A) and subsequently normalized 6 h (D) after receiving LPS (830 µg/Kg i.p., n=6) compared to control (saline, n=6). High magnification images show immunoreactivity for H3S10phK14ac, neuropeptide Y (NPY) (B, E) or glutamic acid decarboxylase (GAD) (C, F) in interneurons of the hippocampus. Merge images show a co-

30

localization between H3S10phK14ac and NPY (B) or GAD (C) at 2 (B, C) but not at 6h (E, F) after LPS injection. Panels G, I and H, J show some Iba1 and GFAP immunoreactive cells, respectively. Two h following LPS treatment no microglial cells and a few astrocytes (red arrows) were H3S10phK14ac immunoreactive as shown by the co-localization of H3S10phK14ac and GFAP immunoreactivity (H); 6 h after LPS injection some Iba1 and GFAP cells co-localize with H3S10phK14ac (red arrows). Scale bar = 50 μm (A, D), 20 μm (G-J), 10 μm (B, C, E, F).

Figure 9. Effect of incubation with LPS on the expression of the pro-inflammatory cytokines IL-1β, IL-6, TNF-α, the enzyme iNOS, the immediate early gene c-Fos, and phospho(S10)-acetylation(K14) of histone H3 in HT-22 and BV-2 cells.

HT-22 and BV-2 cells were treated with LPS (100ng/mL) for 2, 6 or 24 h after which mRNA expression of Interleukin (IL) 1β (A), IL-6 (B), Tumour Necrosis Factor (TNF) α (C), inducible nitric oxide synthase (iNOS) (D), and c-Fos (E), with GAPDH as endogenous control, were measured by Real-time PCR and H3S10phK14ac protein levels (F) were measured in the nuclear extracts by western blot and normalized to total histone H3 levels. Representative blots of H3S10phK14ac and H3 are shown (G). Data are represented as means ± S.E.M. and were analyzed with one-way ANOVA followed by Dunnett's post hoc test. *=p <0.05, **=p<0.01 LPS Vs. control.

Figure 10: Time- and cell-specific effects of LPS on H3S10phK14ac *in vivo* (A) and *in vitro* (B). LPS-activated transcription of the main proinflammatory cytokines and of the inducible isoform of NO synthase was associated with a different pattern of regulation for H3S10phK14ac both in *in vivo* and *in vitro*. Immunohistochemistry data showed that a systemic LPS administration induced a marked region- and cell-specific phospho(S10)-acetylation(K14) of histone H3, characterized by an early and sustained activation of neuronal cells starting as early as after a 2 h exposure and tardive

recruitment of microglia in both the hippocampus and hypothalamus (A). This effect was further confirmed *in vitro*: in the hippocampal cell line HT-22 the phosphoacetylation of histone H3 remained elevated at least until 24 h, while in BV-2 microglial cells an increase was observed starting at 24 h (B).

References

Abd El-Aleem, S., Ragab, S., Ahmed, R., 2008. Upregulation of the Inducible Nitric Oxide Synthase in Rat Hippocampus in A Model of Alzheimer's Disease: A possible Mechanism of Aluminium Induced Alzheimer's 32, 173–180.

Alboni, S., Benatti, C., Montanari, C., Tascedda, F., Brunello, N., 2013a. Chronic antidepressant treatments resulted in altered expression of genes involved in inflammation in the rat hypothalamus. Eur. J. Pharmacol. 721, 158–167. https://doi.org/10.1016/j.ejphar.2013.08.046

Alboni, S., Benatti, C., Montanari, C., Tascedda, F., Brunello, N., 2013b. Chronic antidepressant treatments resulted in altered expression of genes involved in inflammation in the rat hypothalamus. Eur. J. Pharmacol. 721, 158–67. https://doi.org/10.1016/j.ejphar.2013.08.046

Alboni, S., Maggi, L., 2015. Editorial: Cytokines as Players of Neuronal Plasticity and Sensitivity to Environment in Healthy and Pathological Brain. Front. Cell. Neurosci. 9, 508. https://doi.org/10.3389/fncel.2015.00508

Alboni, S., Micioni Di Bonaventura, M.V., Benatti, C., Giuseppponi, M.E., Brunello, N., Cifani, C., 2017. Hypothalamic expression of inflammatory mediators in an animal model of binge eating. Behav. Brain Res. 320, 420–430. https://doi.org/10.1016/j.bbr.2016.10.044

Alboni, S., Montanari, C., Benatti, C., Sanchez-Alavez, M., Rigillo, G., Blom, J.M.C., Brunello, N., Conti, B., Pariante, M.C., Tascedda, F., 2014a. Interleukin 18 activates MAPKs and STAT3 but not NF-κB in hippocampal HT-22 cells. Brain. Behav. Immun. 40, 85–94. https://doi.org/10.1016/j.bbi.2014.02.015

Alboni, S., Montanari, C., Benatti, C., Sanchez-Alavez, M., Rigillo, G., Blom, J.M.C., Brunello, N., Conti, B., Pariante, M.C., Tascedda, F., 2014b. Interleukin 18 activates MAPKs and STAT3 but not NF-κB in hippocampal HT-22 cells. Brain. Behav. Immun. 40, 85–94. https://doi.org/10.1016/j.bbi.2014.02.015

Alboni, S., van Dijk, R.M., Poggini, S., Milior, G., Perrotta, M., Drenth, T., Brunello, N., Wolfer, D.P., Limatola, C., Amrein, I., Cirulli, F., Maggi, L., Branchi, I., 2017. Fluoxetine effects on molecular, cellular and behavioral endophenotypes of depression are driven by the living environment. Mol. Psychiatry 22, 552–561. https://doi.org/10.1038/mp.2015.142

André, C., O'Connor, J.C., Kelley, K.W., Lestage, J., Dantzer, R., Castanon, N., 2008. Spatio-temporal differences in the profile of murine brain expression of proinflammatory cytokines and indoleamine 2,3-dioxygenase in response to peripheral lipopolysaccharide administration. J. Neuroimmunol. 200, 90–9.

Angrisano, T., Lembo, F., Peluso, S., Keller, S., Chiariotti, L., Pero, R., 2012. Helicobacter pylori regulates iNOS promoter by histone modifications in human gastric epithelial cells. Med. Microbiol. Immunol. 201, 249–257. https://doi.org/10.1007/s00430-011-0227-9

Arai, K., Ikegaya, Y., Nakatani, Y., Kudo, I., Nishiyama, N., Matsuki, N., 2001. Phospholipase A $_2$ mediates ischemic injury in the hippocampus: a regional difference of neuronal vulnerability. Eur. J. Neurosci. 13, 2319–2323. https://doi.org/10.1046/j.0953-816x.2001.01623.x

Bagot, R.C., Labonté, B., Peña, C.J., Nestler, E.J., 2014. Epigenetic signaling in psychiatric disorders: stress and depression. Dialogues Clin. Neurosci. 16, 281–95.

Basta-Kaim, A., Budziszewska, B., Leśkiewicz, M., Fijał, K., Regulska, M., Kubera, M., Wędzony, K., Lasoń, W., 2011. Hyperactivity of the hypothalamus-pituitary-adrenal axis in lipopolysaccharide-induced neurodevelopmental model of schizophrenia in rats: effects of antipsychotic drugs. Eur. J. Pharmacol. 650, 586–95. https://doi.org/10.1016/j.ejphar.2010.09.083

Benatti, C., Alboni, S., Blom, J.M.C., Gandolfi, F., Mendlewicz, J., Brunello, N., Tascedda, F., 2014. Behavioural and transcriptional effects of escitalopram in the chronic escape deficit model of depression. Behav. Brain Res. 272, 121–30. https://doi.org/10.1016/j.bbr.2014.06.040

Benatti, C., Alboni, S., Blom, J.M.C., Mendlewicz, J., Tascedda, F., Brunello, N., 2018. Molecular changes associated with escitalopram response in a stress-based model of depression. Psychoneuroendocrinology 87, 74–82. https://doi.org/10.1016/j.psyneuen.2017.10.011

Benatti, C., Alboni, S., Montanari, C., Caggia, F., Tascedda, F., Brunello, N., Blom, J.M.C., 2011. Central effects of a local inflammation in three commonly used mouse strains with a different anxious phenotype. Behav. Brain Res. 224, 23–34. https://doi.org/10.1016/j.bbr.2011.05.011

Benatti, C., Blom, J.M.C., Rigillo, G., Alboni, S., Zizzi, F., Torta, R., Brunello, N., Tascedda, F., 2016. Disease-Induced Neuroinflammation and Depression. CNS Neurol. Disord. Drug Targets 15, 414–33.

Bousiges, O., Neidl, R., Majchrzak, M., Muller, M.-A., Barbelivien, A., Pereira de Vasconcelos, A., Schneider, A., Loeffler, J.-P., Cassel, J.-C., Boutillier, A.-L., 2013. Detection of Histone Acetylation Levels in the Dorsal Hippocampus Reveals Early Tagging on Specific Residues of H2B and H4 Histones in Response to Learning. PLoS One 8, e57816. https://doi.org/10.1371/journal.pone.0057816

Carreira, B.P., Santos, D.F., Santos, A.I., Carvalho, C.M., Araújo, I.M., 2015. Nitric Oxide Regulates Neurogenesis in the Hippocampus following Seizures. Oxid. Med. Cell. Longev. 2015, 451512. https://doi.org/10.1155/2015/451512

Chandramohan, Y., Droste, S.K., Reul, J.M.H.M., 2007. Novelty stress induces phospho-acetylation of histone H3 in rat dentate gyrus granule neurons through coincident signalling via the N-methyl-d-aspartate receptor and the glucocorticoid receptor: relevance for c-fos induction. J. Neurochem. 101, 815–828. https://doi.org/10.1111/j.1471-4159.2006.04396.x

Chen, Y., Sharma, R.P., Costa, R.H., Costa, E., Grayson, D.R., 2002. On the epigenetic regulation of the human reelin promoter. Nucleic Acids Res. 30, 2930–9.

Cherry, J.D., Olschowka, J.A., O'Banion, M., 2014. Neuroinflammation and M2 microglia: the good, the bad, and the inflamed. J. Neuroinflammation 11, 98. https://doi.org/10.1186/1742-2094-11-98

Cheung, P., Tanner, K.G., Cheung, W.L., Sassone-Corsi, P., Denu, J.M., Allis, C.D., 2000. Synergistic coupling of histone H3 phosphorylation and acetylation in response to epidermal growth factor stimulation. Mol. Cell 5, 905–15.

Chuang, Y.-C., Chen, S.-D., Lin, T.-K., Chang, W.-N., Lu, C.-H., Liou, C.-W., Chan, S.H.H., Chang, A.Y.W., 2010. Transcriptional upregulation of nitric oxide synthase II by nuclear factor-κB promotes apoptotic neuronal cell death in the hippocampus following experimental status epilepticus. J. Neurosci. Res. NA-NA. https://doi.org/10.1002/jnr.22369

Chwang, W.B., O'Riordan, K.J., Levenson, J.M., Sweatt, J.D., 2006. ERK/MAPK regulates hippocampal histone phosphorylation following contextual fear conditioning. Learn. Mem. 13, 322–8. https://doi.org/10.1101/lm.152906

Ciccarelli, A., Calza, A., Santoru, F., Grasso, F., Concas, A., Sassoè-Pognetto, M., Giustetto, M., 2013. Morphine withdrawal produces ERK-dependent and ERK-independent epigenetic marks in neurons of the nucleus accumbens and lateral septum. Neuropharmacology 70, 168–179. https://doi.org/10.1016/J.NEUROPHARM.2012.12.010

Claycombe, K.J., Brissette, C.A., Ghribi, O., 2015. Epigenetics of Inflammation, Maternal Infection, and Nutrition1–3. J. Nutr. 145, 1109S–1115S. https://doi.org/10.3945/jn.114.194639

Clayton, A.L., Rose, S., Barratt, M.J., Mahadevan, L.C., 2000. Phosphoacetylation of histone H3 on c-*fos*- and c-*jun*-associated nucleosomes upon gene activation. EMBO J. 19, 3714–3726. https://doi.org/10.1093/emboj/19.14.3714

Collins, A., Hill, L.E., Chandramohan, Y., Whitcomb, D., Droste, S.K., Reul, J.M.H.M., 2009. Exercise Improves Cognitive Responses to Psychological Stress through Enhancement of Epigenetic Mechanisms and Gene Expression in the Dentate Gyrus. PLoS One 4, e4330. https://doi.org/10.1371/journal.pone.0004330

Colvis, C.M., Pollock, J.D., Goodman, R.H., Impey, S., Dunn, J., Mandel, G., Champagne, F.A., Mayford, M., Korzus, E., Kumar, A., Renthal, W., Theobald, D.E.H., Nestler, E.J., 2005. Epigenetic Mechanisms and Gene Networks in the Nervous System. J. Neurosci. 25, 10379–10389. https://doi.org/10.1523/JNEUROSCI.4119-05.2005

Corbett, B.F., You, J.C., Zhang, X., Pyfer, M.S., Tosi, U., Iascone, D.M., Petrof, I., Hazra, A., Fu, C.-H., Stephens, G.S., Ashok, A.A., Aschmies, S., Zhao, L., Nestler, E.J., Chin, J., 2017. ΔFosB Regulates Gene Expression and Cognitive Dysfunction in a Mouse Model of Alzheimer's Disease. Cell Rep. 20, 344–355. https://doi.org/10.1016/j.celrep.2017.06.040

Crosio, C., 2003. Chromatin remodeling and neuronal response: multiple signaling pathways induce specific histone H3 modifications and early gene expression in hippocampal neurons. J. Cell Sci. 116, 4905–4914. https://doi.org/10.1242/jcs.00804

Cunningham, C., 2013. Microglia and neurodegeneration: the role of systemic inflammation. Glia 61, 71–90. https://doi.org/10.1002/glia.22350

da Silva, J.C., Scorza, F.A., Nejm, M.B., Cavalheiro, E.A., Cukiert, A., 2014. c-FOS Expression After Hippocampal Deep Brain Stimulation in Normal Rats. Neuromodulation Technol. Neural Interface 17, 213–217. https://doi.org/10.1111/ner.12122

Damm, J., Wiegand, F., Harden, L.M., Gerstberger, R., Rummel, C., Roth, J., 2012. Fever, sickness behavior, and expression of inflammatory genes in the hypothalamus after systemic and localized subcutaneous stimulation of rats with the toll-like receptor 7 agonist imiquimod. Neuroscience 201, 166–183. https://doi.org/10.1016/J.NEUROSCIENCE.2011.11.013

Dantzer, R., 2009. Cytokine, Sickness Behavior, and Depression. Immunol. Allergy Clin. North Am. 29, 247–264. https://doi.org/10.1016/j.iac.2009.02.002

Dantzer, R., Kelley, K.W., 2007. Twenty years of research on cytokine-induced sickness behavior. Brain. Behav. Immun. 21, 153–160. https://doi.org/10.1016/j.bbi.2006.09.006

Dantzer, R., O'Connor, J.C., Freund, G.G., Johnson, R.W., Kelley, K.W., 2008. From inflammation to sickness and depression: when the immune system subjugates the brain. Nat. Rev. Neurosci. 9, 46–56. https://doi.org/10.1038/nrn2297

Fleischmann, A., Hvalby, O., Jensen, V., Strekalova, T., Zacher, C., Layer, L.E., Kvello, A., Reschke, M., Spanagel, R., Sprengel, R., Wagner, E.F., Gass, P., 2003. Impaired long-term memory and NR2A-type NMDA receptor-dependent synaptic plasticity in mice lacking c-Fos in the CNS. J. Neurosci. 23, 9116–22. https://doi.org/10.1523/JNEUROSCI.23-27-09116.2003

Fletcher, M.A., Rosenthal, M., Antoni, M., Ironson, G., Zeng, X.R., Barnes, Z., Harvey, J.M., Hurwitz, B., Levis, S., Broderick, G., Klimas, N.G., 2010. Plasma neuropeptide Y: a biomarker for symptom severity in chronic fatigue syndrome. Behav. Brain Funct. 6, 76. https://doi.org/10.1186/1744-9081-6-76

Francesconi, W., Sánchez-Alavez, M., Berton, F., Alboni, S., Benatti, C., Mori, S., Nguyen, W., Zorrilla, E., Moroncini, G., Tascedda, F., Conti, B., 2016. The Proinflammatory Cytokine Interleukin 18 Regulates Feeding by Acting on the Bed Nucleus of the Stria Terminalis. J. Neurosci. 36, 5170–5180. https://doi.org/10.1523/JNEUROSCI.3919-15.2016

Frenois, F., Moreau, M., O'Connor, J., Lawson, M., Micon, C., Lestage, J., Kelley, K.W., Dantzer, R., Castanon, N., 2007. Lipopolysaccharide induces delayed FosB/DeltaFosB immunostaining within the mouse extended amygdala, hippocampus and hypothalamus, that parallel the expression of depressive-like behavior. Psychoneuroendocrinology 32, 516–31. https://doi.org/10.1016/j.psyneuen.2007.03.005

Frick, L.R., Williams, K., Pittenger, C., 2013. Microglial dysregulation in psychiatric disease. Clin. Dev. Immunol. 2013, 608654. https://doi.org/10.1155/2013/608654

Gądek-Michalska, A., Tadeusz, J., Rachwalska, P., Bugajski, J., 2013. Cytokines, prostaglandins and nitric oxide in the regulation of stress-response systems. Pharmacol. Rep. 65, 1655–62.

Garden, G.A., 2013. Epigenetics and the modulation of neuroinflammation. Neurotherapeutics 10, 782–8. https://doi.org/10.1007/s13311-013-0207-4

Godbout, J.P., Chen, J., Abraham, J., Richwine, A.F., Berg, B.M., Kelley, K.W., Johnson, R.W., 2005. Exaggerated neuroinflammation and sickness behavior in aged mice following activation of the peripheral innate immune system. FASEB J. 19, 1329–31. https://doi.org/10.1096/fj.05-3776fje

Gore, A.C., 2010. Neuroendocrine targets of endocrine disruptors. Hormones (Athens). 9, 16–27.

Hamon, M.A., Cossart, P., 2008. Histone modifications and chromatin remodeling during bacterial infections. Cell Host Microbe 4, 100–9. https://doi.org/10.1016/j.chom.2008.07.009

Handy, D.E., Castro, R., Loscalzo, J., 2011. Epigenetic Modifications: Basic Mechanisms and Role in Cardiovascular Disease. Circulation 123, 2145–2156. https://doi.org/10.1161/CIRCULATIONAHA.110.956839

He, J., Yamada, K., Nabeshima, T., 2002. A Role of Fos Expression in the CA3 Region of the Hippocampus in Spatial Memory Formation in Rats. Neuropsychopharmacology 26, 259–268. https://doi.org/10.1016/S0893-133X(01)00332-3

Heneka, M.T., Feinstein, D.L., 2001. Expression and function of inducible nitric oxide synthase in neurons. J. Neuroimmunol. 114, 8–18.

Henry, C.J., Huang, Y., Wynne, A.M., Godbout, J.P., 2009. Peripheral lipopolysaccharide (LPS) challenge promotes microglial hyperactivity in aged mice that is associated with exaggerated induction of both pro-inflammatory IL-1β and anti-inflammatory IL-10 cytokines. Brain. Behav. Immun. 23, 309–317. https://doi.org/10.1016/J.BBI.2008.09.002

Hoogland, I.C.M., Houbolt, C., van Westerloo, D.J., van Gool, W.A., van de Beek, D., 2015. Systemic inflammation and microglial activation: systematic review of animal experiments. J. Neuroinflammation 12, 114. https://doi.org/10.1186/s12974-015-0332-6

James, T.T., Aroor, A.R., Lim, R.W., Shukla, S.D., 2012. Histone H3 Phosphorylation (Ser10, Ser28) and Phosphoacetylation (K9S10) Are Differentially Associated with Gene Expression in Liver of Rats Treated In Vivo with Acute Ethanol. J. Pharmacol. Exp. Ther. 340, 237–247. https://doi.org/10.1124/jpet.111.186775

Jin, S., Kim, J.G., Park, J.W., Koch, M., Horvath, T.L., Lee, B.J., 2016. Hypothalamic TLR2 triggers sickness behavior via a microglia-neuronal axis. Sci. Rep. 6, 29424. https://doi.org/10.1038/srep29424

Katashima, C.K., Silva, V.R.R., Lenhare, L., Marin, R.M., Carvalheira, J.B.C., 2017. iNOS promotes hypothalamic insulin resistance associated with deregulation of energy balance and obesity in rodents. Sci. Rep. 7, 9265. https://doi.org/10.1038/s41598-017-08920-z

Kloss, C.U., Werner, A., Klein, M.A., Shen, J., Menuz, K., Probst, J.C., Kreutzberg, G.W., Raivich, G., 1999. Integrin family of cell adhesion molecules in the injured brain: regulation and cellular localization in the normal and regenerating mouse facial motor nucleus. J. Comp. Neurol. 411, 162–78.

Kumar, A., Choi, K.-H., Renthal, W., Tsankova, N.M., Theobald, D.E.H., Truong, H.-T., Russo, S.J., Laplant, Q., Sasaki, T.S., Whistler, K.N., Neve, R.L., Self, D.W., Nestler, E.J., 2005. Chromatin remodeling is a key mechanism underlying cocaine-induced plasticity in striatum. Neuron 48, 303–14. https://doi.org/10.1016/j.neuron.2005.09.023

Lawson, M.A., Parrott, J.M., McCusker, R.H., Dantzer, R., Kelley, K.W., O'Connor, J.C., 2013.

Intracerebroventricular administration of lipopolysaccharide induces indoleamine-2,3-dioxygenase-dependent depression-like behaviors. J. Neuroinflammation 10, 875. https://doi.org/10.1186/1742-2094-10-87

Layé, S., Parnet, P., Goujon, E., Dantzer, R., 1994. Peripheral administration of lipopolysaccharide induces the expression of cytokine transcripts in the brain and pituitary of mice. Brain Res. Mol. Brain Res. 27, 157–62.

Luo, C.X., Zhu, X.J., Zhou, Q.G., Wang, B., Wang, W., Cai, H.H., Sun, Y.J., Hu, M., Jiang, J., Hua, Y., Han, X., Zhu, D.Y., 2007. Reduced neuronal nitric oxide synthase is involved in ischemia-induced hippocampal neurogenesis by up-regulating inducible nitric oxide synthase expression. J. Neurochem. 103, 1872–1882. https://doi.org/10.1111/j.1471-4159.2007.04915.x

Lupien, S.J., McEwen, B.S., Gunnar, M.R., Heim, C., 2009. Effects of stress throughout the lifespan on the brain, behaviour and cognition. Nat. Rev. Neurosci. 10, 434–445. https://doi.org/10.1038/nrn2639

Lynch, M.A., 2002. Interleukin-1 beta exerts a myriad of effects in the brain and in particular in the hippocampus: analysis of some of these actions. Vitam. Horm. 64, 185–219.

Madabhushi, R., Gao, F., Pfenning, A.R., Pan, L., Yamakawa, S., Seo, J., Rueda, R., Phan, T.X., Yamakawa, H., Pao, P.-C., Stott, R.T., Gjoneska, E., Nott, A., Cho, S., Kellis, M., Tsai, L.-H., 2015. Activity-Induced DNA Breaks Govern the Expression of Neuronal Early-Response Genes. Cell 161, 1592–1605. https://doi.org/10.1016/J.CELL.2015.05.032

Matt, S.M., Lawson, M.A., Johnson, R.W., 2016. Aging and peripheral lipopolysaccharide can modulate epigenetic regulators and decrease IL-1β promoter DNA methylation in microglia. Neurobiol. Aging 47, 1–9. https://doi.org/10.1016/j.neurobiolaging.2016.07.006

McCann, S.M., Kimura, M., Karanth, S., Yu, W.H., Rettori, V., 1997. Nitric Oxide Controls the Hypothalamic-Pituitary Response to Cytokines. Neuroimmunomodulation 4, 98–106. https://doi.org/10.1159/000097327

McClain, J.A., Nixon, K., 2016. Alcohol Induces Parallel Changes in Hippocampal Histone H3 Phosphorylation and c-Fos Protein Expression in Male Rats. Alcohol. Clin. Exp. Res. 40, 102–12. https://doi.org/10.1111/acer.12933

McClung, C.A., Nestler, E.J., 2008. Neuroplasticity Mediated by Altered Gene Expression. Neuropsychopharmacology 33, 3–17. https://doi.org/10.1038/sj.npp.1301544

Mifsud, K.R., Gutièrrez-Mecinas, M., Trollope, A.F., Collins, A., Saunderson, E.A., Reul, J.M.H.M., 2011. Epigenetic mechanisms in stress and adaptation. Brain. Behav. Immun. 25, 1305–1315. https://doi.org/10.1016/j.bbi.2011.06.005

Moraes, J.C., Amaral, M.E., Picardi, P.K., Calegari, V.C., Romanatto, T., Bermúdez-Echeverry, M., Chiavegatto, S., Saad, M.J., Velloso, L.A., 2006. Inducible-NOS but not neuronal-NOS participate in the acute effect of TNF-α on hypothalamic insulin-dependent inhibition of food intake. FEBS Lett. 580, 4625–4631.

https://doi.org/10.1016/J.FEBSLET.2006.07.042

Mori, T., Wakabayashi, T., Ogawa, H., Hirahara, Y., Koike, T., Yamada, H., 2013. Increased histone H3 phosphorylation in neurons in specific brain structures after induction of status epilepticus in mice. PLoS One 8, e77710. https://doi.org/10.1371/journal.pone.0077710

Nabavi, S.F., Braidy, N., Orhan, I.E., Badiee, A., Daglia, M., Nabavi, S.M., 2016. Rhodiola rosea L. and Alzheimer's Disease: From Farm to Pharmacy. Phyther. Res. 30, 532–539. https://doi.org/10.1002/ptr.5569

Nestler, E.J., 2014. Epigenetic mechanisms of depression. JAMA psychiatry 71, 454–6. https://doi.org/10.1001/jamapsychiatry.2013.4291

Norden, D.M., Trojanowski, P.J., Villanueva, E., Navarro, E., Godbout, J.P., 2016. Sequential activation of microglia and astrocyte cytokine expression precedes increased Iba-1 or GFAP immunoreactivity following systemic immune challenge. Glia 64, 300–16. https://doi.org/10.1002/glia.22930

Nowak, S.J., Corces, V.G., 2000. Phosphorylation of histone H3 correlates with transcriptionally active loci. Genes Dev. 14, 3003–13.

Olsson, E.M., von Schéele, B., Panossian, A.G., 2009. A randomised, double-blind, placebo-controlled, parallel-group study of the standardised extract shr-5 of the roots of Rhodiola rosea in the treatment of subjects with stress-related fatigue. Planta Med. 75, 105–12. https://doi.org/10.1055/s-0028-1088346

Ottaviani, E., Accorsi, A., Rigillo, G., Malagoli, D., Blom, J.M.C., Tascedda, F., 2013. Epigenetic modification in neurons of the mollusc Pomacea canaliculata after immune challenge. Brain Res. 1537, 18–26. https://doi.org/10.1016/j.brainres.2013.09.009

Petrov, T., Page, A.B., Owen, C.R., Rafols, J.A., 2000. Expression of the inducible nitric oxide synthase in distinct cellular types after traumatic brain injury: an in situ hybridization and immunocytochemical study. Acta Neuropathol. 100, 196–204.

Qin, L., Wu, X., Block, M.L., Liu, Y., Breese, G.R., Hong, J.-S., Knapp, D.J., Crews, F.T., 2007. Systemic LPS causes chronic neuroinflammation and progressive neurodegeneration. Glia 55, 453–62. https://doi.org/10.1002/glia.20467

Raivich, G., Jones, L.L., Werner, A., Blüthmann, H., Doetschmann, T., Kreutzberg, G.W., 1999. Molecular signals for glial activation: pro- and anti-inflammatory cytokines in the injured brain. Acta Neurochir. Suppl. 73, 21–30.

Rea, S., Eisenhaber, F., O'Carroll, D., Strahl, B.D., Sun, Z.-W., Schmid, M., Opravil, S., Mechtler, K., Ponting, C.P., Allis, C.D., Jenuwein, T., 2000. Regulation of chromatin structure by site-specific histone H3 methyltransferases. Nature 406, 593–599. https://doi.org/10.1038/35020506

Ribeiro, D.E., Maiolini, V.M., Soncini, R., Antunes-Rodrigues, J., Elias, L.L.K., Vilela, F.C., Giusti-Paiva, A., 2013. Inhibition of nitric oxide synthase accentuates endotoxin-induced sickness behavior in mice. Pharmacol.

Biochem. Behav. 103, 535–540. https://doi.org/10.1016/J.PBB.2012.09.022

Rodrigo, J., Alonso, D., Fernández, A.P., Serrano, J., Richart, A., López, J.C., Santacana, M., Martínez-Murillo, R., Bentura, M.L., Ghiglione, M., Uttenthal, L.O., 2001. Neuronal and inducible nitric oxide synthase expression and protein nitration in rat cerebellum after oxygen and glucose deprivation. Brain Res. 909, 20–45.

Ryabinin, A.E., Criado, J.R., Henriksen, S.J., Bloom, F.E., Wilson, M.C., 1997. Differential sensitivity of c-Fos expression in hippocampus and other brain regions to moderate and low doses of alcohol. Mol. Psychiatry 2, 32–43.

Saccani, S., Pantano, S., Natoli, G., 2002. p38-dependent marking of inflammatory genes for increased NF-κB recruitment. Nat. Immunol. 3, 69–75. https://doi.org/10.1038/ni748

Satta, M.A., Jacobs, R.A., Kaltsas, G.A., Grossman, A.B., 1998. Endotoxin induces interleukin-1beta and nitric oxide synthase mRNA in rat hypothalamus and pituitary. Neuroendocrinology 67, 109–16.

Sawicka, A., Seiser, C., 2012. Histone H3 phosphorylation – A versatile chromatin modification for different occasions. Biochimie 94, 2193–2201. https://doi.org/10.1016/J.BIOCHI.2012.04.018

Scientific Opinion on the substantiation of a health claim related to *Rhodiola rosea* L. extract and reduction of mental fatigue pursuant to Article 13(5) of Regulation (EC) No 1924/2006, 2012. . EFSA J. 10, 2805. https://doi.org/10.2903/j.efsa.2012.2805

Sens, J., Schneider, E., Mauch, J., Schaffstein, A., Mohamed, S., Fasoli, K., Saurine, J., Britzolaki, A., Thelen, C., Pitychoutis, P.M., 2017. Lipopolysaccharide administration induces sex-dependent behavioural and serotonergic neurochemical signatures in mice. Pharmacol. Biochem. Behav. 153, 168–181. https://doi.org/10.1016/j.pbb.2016.12.016

Sierra, A., Gottfried-Blackmore, A.C., McEwen, B.S., Bulloch, K., 2007. Microglia derived from aging mice exhibit an altered inflammatory profile. Glia 55, 412–424. https://doi.org/10.1002/glia.20468

Soloaga, A., Thomson, S., Wiggin, G.R., Rampersaud, N., Dyson, M.H., Hazzalin, C.A., Mahadevan, L.C., Arthur, J.S.C., 2003. MSK2 and MSK1 mediate the mitogen- and stress-induced phosphorylation of histone H3 and HMG-14. EMBO J. 22, 2788–97. https://doi.org/10.1093/emboj/cdg273

Taniura, H., Sng, J.C.G., Yoneda, Y., 2006. Histone modifications in status epilepticus induced by kainate. Histol. Histopathol. 21, 785–91. https://doi.org/10.14670/HH-21.785

Thompson, S.L., Konfortova, G., Gregory, R.I., Reik, W., Dean, W., Feil, R., 2001. Environmental effects on genomic imprinting in mammals. Toxicol. Lett. 120, 143–150. https://doi.org/10.1016/S0378-4274(01)00292-2

Thomson, S., Clayton, A.L., Hazzalin, C.A., Rose, S., Barratt, M.J., Mahadevan, L.C., 1999. The nucleosomal response associated with immediate-early gene induction is mediated via alternative MAP kinase cascades: MSK1 as a potential histone H3/HMG-14 kinase. EMBO J. 18, 4779–4793. https://doi.org/10.1093/emboj/18.17.4779

Tischmeyer, W., Grimm, R., 1999. Activation of immediate early genes and memory formation. Cell. Mol. Life Sci. 55, 564–574. https://doi.org/10.1007/s000180050315

Tsankova, N.M., Kumar, A., Nestler, E.J., 2004. Histone Modifications at Gene Promoter Regions in Rat Hippocampus after Acute and Chronic Electroconvulsive Seizures. J. Neurosci. 24, 5603–5610. https://doi.org/10.1523/JNEUROSCI.0589-04.2004

Uribe, R.M., Lee, S., Rivier, C., 1999. Endotoxin stimulates nitric oxide production in the paraventricular nucleus of the hypothalamus through nitric oxide synthase I: correlation with hypothalamic-pituitary-adrenal axis activation. Endocrinology 140, 5971–81. https://doi.org/10.1210/endo.140.12.7170

Vilella, A., Tosi, G., Grabrucker, A.M., Ruozi, B., Belletti, D., Vandelli, M.A., Boeckers, T.M., Forni, F., Zoli, M., 2014. Insight on the fate of CNS-targeted nanoparticles. Part I: Rab5-dependent cell-specific uptake and distribution. J. Control. Release 174, 195–201. https://doi.org/10.1016/j.jconrel.2013.11.023

von Bernhardi, R., Eugenín-von Bernhardi, L., Eugenín, J., 2015. Microglial cell dysregulation in brain aging and neurodegeneration. Front. Aging Neurosci. 7, 124. https://doi.org/10.3389/fnagi.2015.00124

Watson, L.A., Tsai, L.-H., 2017. In the loop: how chromatin topology links genome structure to function in mechanisms underlying learning and memory. Curr. Opin. Neurobiol. 43, 48–55. https://doi.org/10.1016/J.CONB.2016.12.002

Weaver, I.C.G., Cervoni, N., Champagne, F.A., D'Alessio, A.C., Sharma, S., Seckl, J.R., Dymov, S., Szyf, M., Meaney, M.J., 2004. Epigenetic programming by maternal behavior. Nat. Neurosci. 7, 847–54. https://doi.org/10.1038/nn1276

Yuste, J.E., Tarragon, E., Campuzano, C.M., Ros-Bernal, F., 2015. Implications of glial nitric oxide in neurodegenerative diseases. Front. Cell. Neurosci. 9, 322. https://doi.org/10.3389/fncel.2015.00322

Zhou, Z., Yuan, Q., Mash, D.C., Goldman, D., 2011. Substance-specific and shared transcription and epigenetic changes in the human hippocampus chronically exposed to cocaine and alcohol. Proc. Natl. Acad. Sci. U. S. A. 108, 6626–31. https://doi.org/10.1073/pnas.1018514108

Table 1: Transcript and sequence of each primer used in real time PCR and ChIP assays.

Transcript	NCBI GenBank	Primer sequence
For Real Time PCR in vivo		
IL-1β	NM_031512.2	Fw ACTCGTGGGATGATGACGA Rv TCACATGGGTCAGACAGCAC
IL-6	NM_012589.1	Fw CTTCACAAGTCGGAGGCTTA Rv AGTGCATCATCGCTGTTCAT
TNF-α	NM_012675.3	Fw CCACCACGCTCTTCTGTCTA Rv TGATCTGAGTGTGAGGGTCTG
iNos	NM_012611	Fw ACTTTTAGAGACGCTTCTGAG Rv CATGTCTGTGACTTTGTTGC
c-Fos	NM_022197	Fw CACTCCAAGCGGAGACAGAT Rv GGCTGCCAAAATAAACTCCA

GAPDH	NM_017008.3	Fw CAAGGTCATCCATGACAACTTTG
		Rv GGGCCATCCACAGTCTTCTG

For Real Time PCR in vitro

IL-1β	NM_008361.4	Fw TGAAAGCTCTCCACCTCAATG
		Rv CCAAGGCCACAGGTATTTTG
IL-6	NM_031168.2	Fw CTTCACAAGTCGGAGGCTTA
		Rv CAAGTGCATCATCGTTGTTC
TNF-α	NM_013693.3	Fw GGCCTCCCTCTCATCAGTTC
		Rv CACTTGGTGGTTTGCTACGA
iNos	NM_010927.4	Fw ACGAGACGGATAGGCAGAGA
		Rv GAGTAGTAGCGGGGCTTCAA
c-Fos	NM_010234.2	Fw CACTCCAAGCGGAGACAGAT
		Rv GGCTGCCAAAATAAACTCCA
GAPDH	NM_001289726.1	Fw CAAGGTCATCCATGACAACTTTG
		Rv GGGCCATCCACAGTCTTCTG

For Chip Assay

IL-1β promoter	NC_005102.3	Fw TCAGGACTTAAATGTTCAGC
		Rv AAGGGGTGGCAGACTATGAC
IL-6 promoter	NC_005103.3	Fw CCCACCCTCCAACAAAGAT
		Rv ACAGACATCCCCAGTCTCATA
iNos promoter	NC_005109.3	Fw CCACTATGCTGCCCAAACTA
		Rv CCAGGTTCCAAATGACCAGT
c-Fos promoter	NC_005105.3	Fw AACCATCCCCGAAATCCTA
		Rv GAGCGGAACAGAGAAACTGG

Abbreviations: IL: Interleukin; TNF: Tumor Necrosis Factor; IFN: Interferon; iNOS: inducible NO Synthase; GAPDH: Glyceraldehydes-3-Phosphate Dehydrogenase

Highlights:

- LPS regulates H3 phospho(Ser10)-acetylation(Lys14) (H3S10phK14ac) in the rat brain

- Hippocampal and hypothalamic H3S10phK14ac increase after LPS is time- and area-specific

- iNOS expression is one of the transcriptional effects of LPS regulated by H3S10phK14ac

- LPS-induced increase in H3S10phK14ac occurs mainly in neurons and reactive microglia